

Control of Radiant Cooling Systems for the Honda Smart Home

University of California, Berkeley
May 6th, 2016

Jonathan Woolley, Ann Dennis
UC Berkeley Center for the Built Environment, Department of Architecture
CE 295 - Energy Systems and Control, Professor Moura

TABLE OF CONTENTS

Acknowledgements	2
Abstract.....	3
Introduction.....	4
Technical Description.....	8
<i>Project Methodology</i>	8
Schematic of the System.....	10
Assumptions.....	11
Definition of Parameters and Variables.....	12
<i>Dynamic System Equations</i>	15
Differential Representation.....	15
State Space Representation.....	16
Linear in the Parameters Representation.....	17
<i>Parameter Identification</i>	18
<i>Baseline Conditions</i>	19
<i>Project Results</i>	20
Parameter Identification.....	22
Validation of Dynamical Equations.....	24
Conclusions.....	27
References	28

ACKNOWLEDGEMENTS

We appreciate the input and support on a number of individuals and teams who contributed to this project. Michael Koenig from Honda American Motor company provided insight and guidance about the home. Davis Energy Group and UC Davis provided more than two years of measurement data for our use. In particular, recognition is to due to Daniel Stuart from Davis Energy Group, and Jose Garcia and Caton Mande from UC Davis, who provided preliminary data organization and analysis that laid the foundation for our work on parameter recognition and dynamic simulation.

ABSTRACT

The Honda Smart Home is a zero net energy research and demonstration project that incorporates a variety of innovative energy efficiency design strategies and controls. The study reported herein focuses on control of the primary active cooling systems for the home - a radiant slab on the first floor and radiant ceiling on the second floor. Despite the fact that numerous studies have previously indicated that radiant cooling can use substantially less electricity than conventional forced-air cooling strategies, performance data from occupied operation of the home in 2015 revealed that the system used far more electricity than design models projected. The discrepancy appears to stem from the fact that the heat pump operates for more hours than anticipated and delivers more cooling than annual load calculations predicted. It is likely that several factors contribute to the poor performance, but that the radiant cooling control strategy implemented in the home is at least partly responsible. The study discussed here developed a simplified state-space representation of the systems, then used measured performance data to identify characteristic model parameters. The identified model was compared against an out-of-sample data set to assess its ability to predict system states. Although we were not able to do so in the course of this project, the useful purpose of this model would be to simulate the physical system dynamics with alternate control strategies in order to identify a simple approach to manage the dynamic thermal system more appropriately.

INTRODUCTION

MOTIVATION AND BACKGROUND

The U.S. is responsible for 19% of global annual primary energy consumption, 41% of this energy is consumed in the buildings sector, roughly half of which is used in residential buildings. In aggregate, cooling and heating is responsible for more than half of the site energy consumption for residential buildings (DOE 2012). Efficiency for these mechanical systems has enormous potential to reduce our energy consumption, energy expenses, and environmental footprint. The majority of cooling in residential buildings is provide by simple split type air cooled vapor compression air conditioners. Heating technologies vary largely by region, in California gas furnaces are nearly ubiquitous for residential space heating. In the Pacific Northwest where the development of energy infrastructure was guided largely by the availability of low cost hydroelectric, heating is often provided by electric resistance. The efficiency for cooling and heating systems have been very slow to improve, especially compared to modern advancements in other end use sectors such as lighting, appliances, and electronics.

Many studies have suggested that radiant cooling can use significantly less energy than conventional forced air cooling systems. The advantage is attributed to improved energy conversion efficiency, improved distribution efficiency, and improved efficacy in the way that radiant cooling removes heat from a space and in the way that actively cooled surfaces affect occupant comfort. The buildings industry is beginning to adopt radiant cooling in both residential and commercial settings, but the strategy faces a number of challenges. The present study focuses on control of radiant cooling, which is one of the more substantial technical barriers to broader adoption of the technology. Some major challenges related to control of radiant cooling include:

- Large time constants mean that conventional reactive thermostat control strategies may fail to respond quickly enough to maintain desired room temperature conditions
- Large capacitance of the slab and building mass offer an opportunity for energy storage, such as through nighttime precooling, but since thermal mass is coupled to the occupied conditioned space, the timing of charge and release of thermal energy are highly constrained.
- Radiant cooling affects human thermal comfort differently than forced air cooling, so conventional thermostat set point temperatures may not represent comfort needs properly.
- Slow system response can make it difficult to coordinate radiant cooling with other system modes and efficiency strategies such as natural ventilation cooling or occupancy responsive control.

The project described herein utilized measured performance data from the Honda Smart Home - a positive energy residence and living laboratory at UC Davis - to explore the dynamic thermal behavior of radiant cooling systems. Mechanical cooling for the radiant systems in the Honda Smart Home is generated by a multi-function water-to-water ground-coupled heat pump which operates with COP = 2-6 and which recovers waste heat from cooling for domestic hot water.

The major challenge for control of this system is in aligning the heat pump control input (ON/OFF) with its effect on the conditioned environment. Currently, the heat pump is activated when the room temperature rises above a user selected set point, and operates continuously until the room temperature drops below the set point. Since the radiant slab has a large thermal time constant 6-16 hours may pass between the time that the heat pump is activated and the time that the room returns to the set point. By this time, the mass has been overcooled, the room drifts well below the desired temperature, and the opportunity for natural ventilation cooling in the evening is precluded. These dynamics result in excessive energy use and poor thermal comfort.

PROJECT OBJECTIVES

The primary objective of our project was to develop a state-space model of the radiant cooling systems in the Honda Smart Home that could be used to assess alternate control strategies for these systems.

IMAGES OF HONDA SMART HOME



Figure: North view of Honda Smart Home

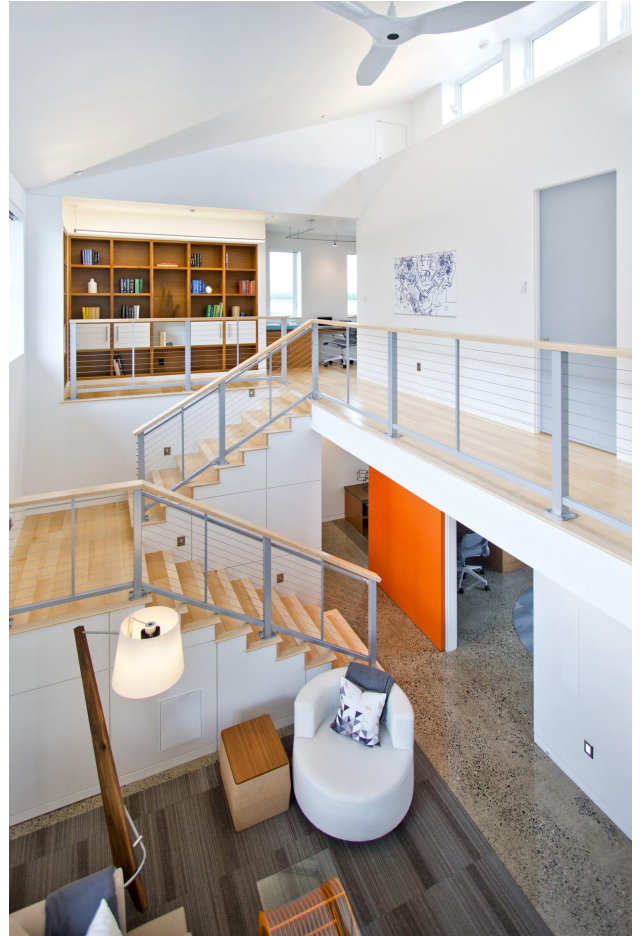


Figure: (Left) Mechanical room, including (from left to right) manifolded domestic hot and cold water distribution system, domestic hot water storage, hydronic plumbing, and water-to-water heat pump. (Right) Greatroom, including radiant slab on the first floor, and radiant ceiling (with ceiling fans) on the second floor.

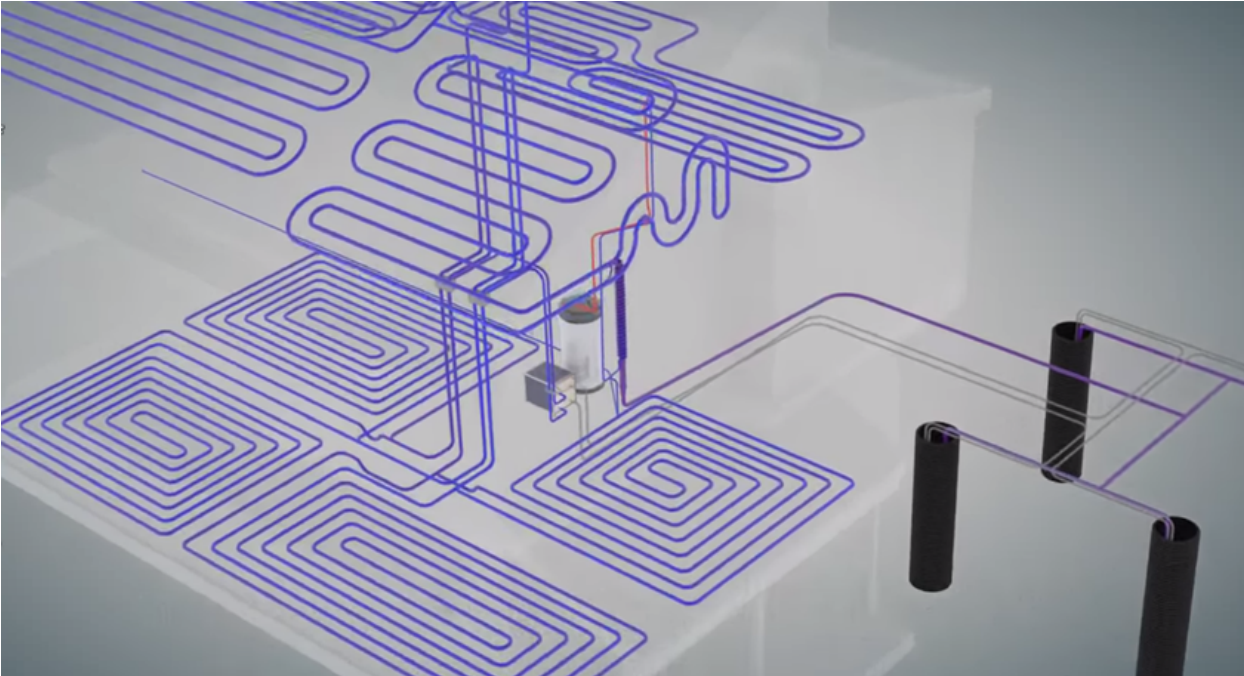


Figure: Animated cut-away of mechanical systems including: ground source heat pump, drainwater heat recovery, radiant floors and radiant ceilings. Animation available online at www.hondasmarthome.com

RELEVANT LITERATURE ON RADIANT COOLING

1. ASHRAE Handbook. HVAC Systems and Equipment 2012. Chapter 13. Hydronic Heating and Cooling.
2. ASHRAE Handbook. HVAC Systems and Equipment 2008. Chapter 12. Hydronic Heating and Cooling System Design.
3. Ferkl, Lukáš, and Jan Široký. 2010. "Ceiling Radiant Cooling: Comparison of ARMAX and Subspace Identification Modelling Methods." *Building and Environment* 45 (1): 205–12.
4. Prívar, Samuel, Jan Široký, Lukáš Ferkl, and Jiří Cigler. 2011. "Model Predictive Control of a Building Heating System: The First Experience." *Energy and Buildings* 43 (2-3): 564–72.
5. Stetiu, Corina. 1999. "Energy and Peak Power Savings Potential of Radiant Cooling Systems in US Commercial Buildings." *Energy and Buildings* 30 (2): 127–38.
6. Afram, Abdul, and Farrokh Janabi-Sharifi. 2014. "Theory and Applications of HVAC Control Systems – A Review of Model Predictive Control (MPC)." *Building and Environment* 72 (February): 343–55. doi:10.1016/j.buildenv.2013.11.016.

TECHNICAL DESCRIPTION

Our project objective is to develop a state space model of the radiant cooling system at the Honda Smart Home and further study the model to resolve current challenges in control schemes. We used measured data to identify model parameters values and validated the dynamic model against out of sample measurements.

PROJECT METHODOLOGY

We began with a schematic of the system that is comprised of 11 nodes with thermal capacitance and links to each adjacent node, where each link is characterized by a linear resistance to heat transfer. The model assumes the various modeling decisions outlined in this report, such as internal gains from occupants is not included. Following the heat flow from node to node as the positive convention, we wrote dynamic equations based on the conservation of energy. Formulated from the first law of thermodynamics and thus a white-box model, this method is useful to us because it can accurately predict states outside of our training data. We rearranged the equations into linear in the parameters form following *CE295 Chapter 2* course notes.

We tested for identifiability of our parameters using persistence of excitation code in Matlab. We compared a condensed “2D” formulation and an expanded “3D” version for ϕ . Table 1 shows results for the slab surface node. Both formulations converge and are identifiable as the persistence of excitation test provided a value greater than zero. PE level for 2D version is “easier” to identify shown by its larger value. As seen in the 3D version, the third element is algebraically related to the first two elements. Grouping the ϕ in the 2D form, prevents overparameterization and is therefore the procedure we chose for all of our dynamical equations.

We identified our parameters with a one-month training data set. In MatLab, we coded a least squares algorithm with forgetting factor for each dynamic equation. We identified the parameters in our system model with a one-month training data set and refined their convergence with tailored forgetting factor, β , update gain, Υ , and initial guesses, θ_0 . We found a forgetting factor $1e-10$ to be the most optimal, where is closer to the pure LSQ or discounts the past less, than a β of $1e-1$. Our initial guesses along with parameter estimation is outlined in Table 3.

We formulated our 11 dynamic equations into state space representation and simulated the model with a one-month out of sample data set. From there, we iteratively improved our parameter estimates. More iterations by plugging in theta results as initial guesses would further improve our model. One method of note in this step was to confirm the parameters are identified with the appropriate sign given the energy balance of our system. We then compared simulation results to the measured states in the Honda Smart Home out of sample data set.

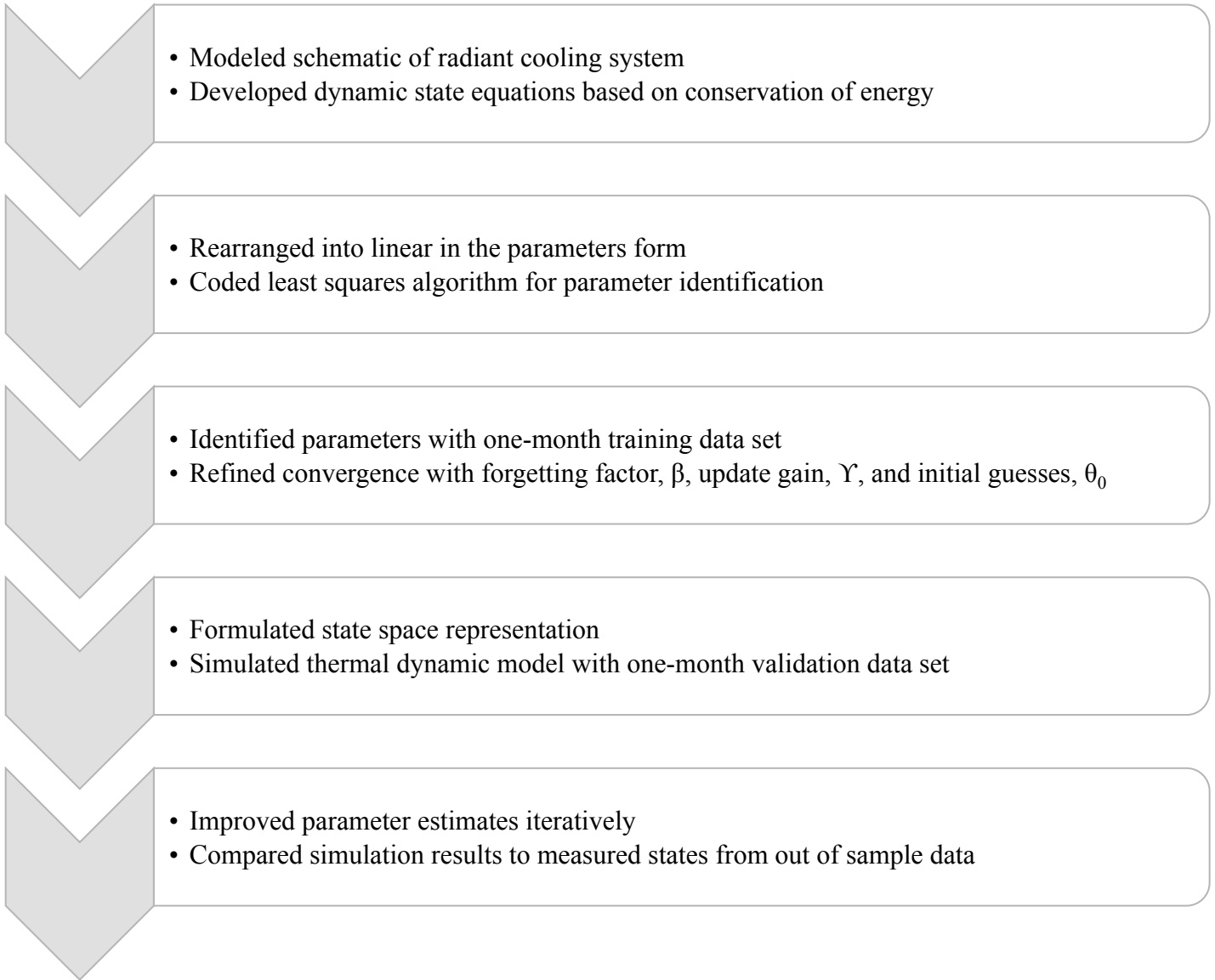


Table 1. Identifiability Test Example: Temperature of Slab Surface

$\text{phi2D} = [T_{Z1} - T_{SS}, T_{SS} - T_{SB}]'$;
 $\text{phi3D} = [T_{Z1}, T_{SS}, T_{SB}]'$;

PE Level for 2D Version : 0.2070
 PE Level for 3D Version : 0.0845

SCHEMATIC OF THE SYSTEM

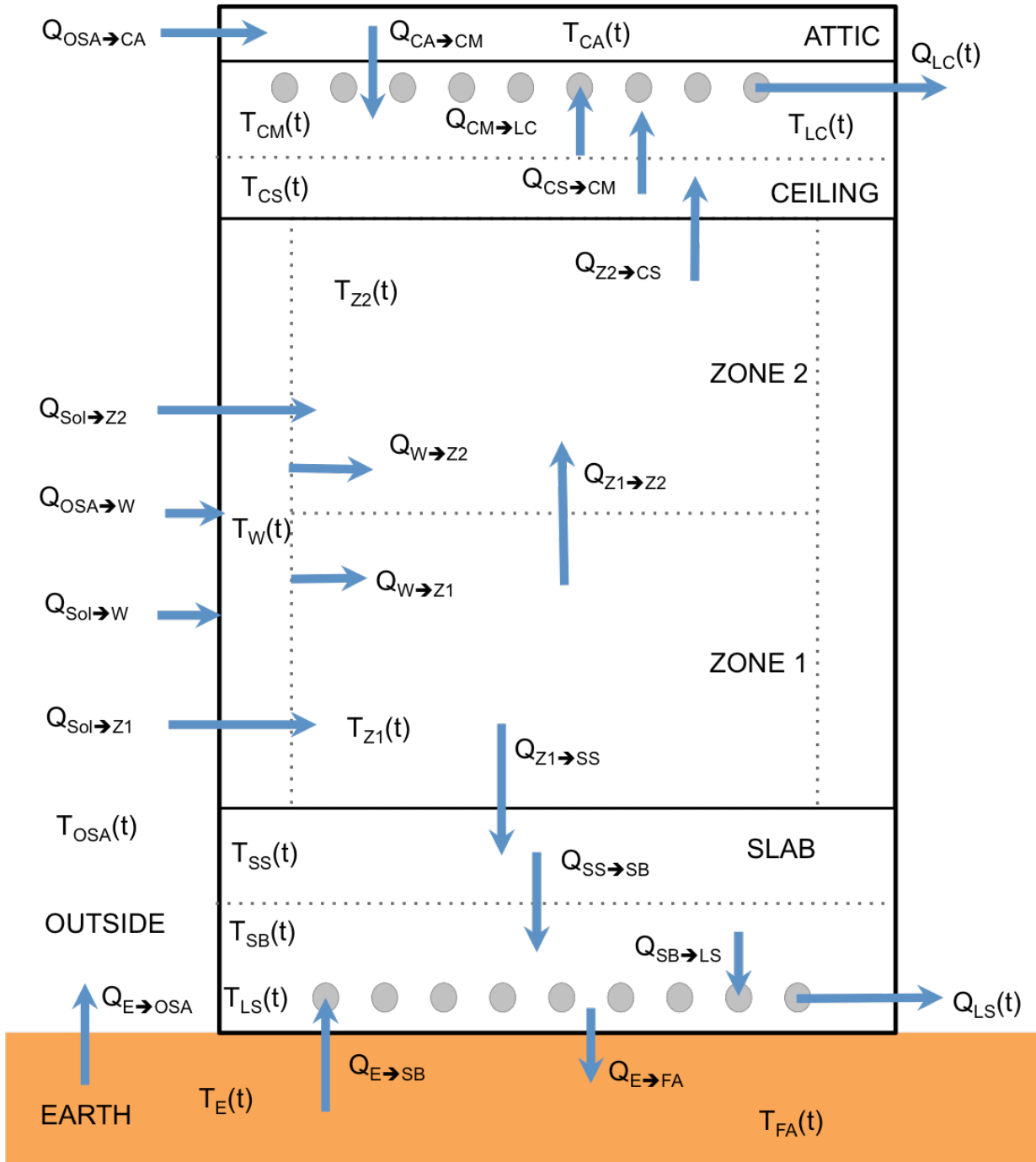


Figure: The schematic of our model: radiant cooling in the Honda Smart Home. $Q_{X \rightarrow X}$ represents heat transfer rate from node to node. Our states and inputs, $T_x(t)$ and $Q_x(t)$ represents temperature and thermal capacity of the node, respectively.

ASSUMPTIONS

We made the following assumptions in creating our model of the Honda Smart Home radiant cooling.

- Internal gains, such as from people and electronics, are not included
- Dynamics associated with interior radiation and convection are ignored
- Heat transfer between reservoirs is modeled as simple 1D conduction
- Thermal capacitance of building components are lumped into convenient groups, for example, all walls represented as a single reservoir
- Interior masses and divisioning, such as interior walls, are not modeled
- Interior space is divided into two zones that are in thermal contact
- Material incongruencies, such as multi layered construction, is not addressed except for where we have measured data to inform the model about states at these points
- The hydronic cooling circuit is modeled as a fluid mass with a single temperature, which will be represented as the average of the load supply and load return temperature at the heat pump.
- Thermal capacity of the heat pump is considered a controlled input, so the dynamic response of the heat pump and the ground coupled heat exchanger is not a part of this model

DEFINITION OF PARAMETERS AND VARIABLES

The following states, inputs, and parameters are identified below in Table 2 with standard notation and units.

STATES			
Load circuit (slab)	T_{LS}	°F	Temperature of water in the load circuit
Earth Below Slab	T_{LE}	°F	Temperature of earth below slab
Slab bottom	T_{SB}	°F	Temperature of slab bottom
Slab surface	T_{SS}	°F	Temperature of slab surface
Zone 1	T_{Z1}	°F	Temperature of zone 1
Walls	T_W	°F	Temperature of walls
Zone 2	T_{Z2}	°F	Temperature of zone 2
Ceiling surface	T_{CS}	°F	Temperature of the ceiling surface
Ceiling middle	T_{CM}	°F	Temperature of ceiling middle
Attic	T_{CA}	°F	Temperature in the attic
Load circuit (ceiling)	T_{LC}	°F	Temperature of water in the load circuit
CONTROLLED INPUTS			
Slab hydronic loop thermal capacity	Q_{LS}	kW	Thermal capacity input to floor
Ceiling hydronic loop thermal capacity	Q_{LC}	kW	Thermal capacity input to ceiling hydronic loop
UNCONTROLLED INPUTS			

Outside	T_{OSA}	°F	Temperature of outside air
Outside	F_{sol}	-	Solar Insolation
Far Earth	T_{FA}	°F	Temperature of the deep earth (constant)
PARAMETERS			
Load circuit (slab)	C_{LS}	E/T	Capacitance of the slab load circuit
Slab bottom to load circuit (slab) interface	$R_{SB \rightarrow LS}$	T/E/time	Total thermal resistance between slab bottom and slab load circuit
Earth Below Slab	C_E	E/T	Capacitance of earth below slab
Earth to outside interface	$R_{E \rightarrow OSA}$	T/E/time	Total thermal resistance between earth below slab and outside air
Earth to far earth interface	$R_{E \rightarrow FA}$	T/E/time	Total thermal resistance between earth below slab and far earth
Earth to slab bottom interface	$R_{E \rightarrow SB}$	T/E/time	Total thermal resistance between earth and slab bottom
Slab bottom	C_{SB}	E/T	Capacitance of slab bottom
Slab surface to slab bottom interface	$R_{SS \rightarrow SB}$	T/E/time	Total thermal resistance between slab surface and slab bottom
Slab surface	C_{SS}	E/T	Capacitance of slab surface
Zone 1 to slab surface interface	$R_{Z1 \rightarrow SS}$	T/E/time	Total thermal resistance between zone 1 and slab surface
Zone 1	C_{Z1}	E/T	Capacitance of zone 1
Zone 1 to zone 2 interface	$R_{Z1 \rightarrow Z2}$	T/E/time	Total thermal resistance between zone 1 and zone 2
Walls to zone 1 interface	$R_{W \rightarrow Z1}$	T/E/time	Total thermal resistance between walls and zone 1

Walls	C_W	E/T	Capacitance of walls
Zone 2	C_{Z2}	E/T	Capacitance of zone 2
Zone 2 to ceiling interface	$R_{Z2 \rightarrow CS}$	T/E/time	Total thermal resistance between zone 2 and ceiling surface
Walls to zone 2 interface	$R_{W \rightarrow Z2}$	T/E/time	Total thermal resistance between walls and zone 2
Ceiling surface (interior surface)	C_{CS}	E/T	Capacitance of the ceiling surface
Ceiling surface to ceiling middle interface	$R_{CS \rightarrow CM}$	T/E/time	Total thermal resistance between ceiling surface and ceiling middle
Ceiling middle (between sheet rock and insulation)	C_{CM}	E/T	Capacitance of the ceiling middle
Attic to ceiling middle interface	$R_{CA \rightarrow CM}$	T/E/time	Total thermal resistance between attic and ceiling middle
Attic (ceiling above insulation)	C_{CA}	E/T	Capacitance of "attic" (and roof construction) above the ceiling insulation
Load Circuit (ceiling)	C_{LC}	E/T	Capacitance of load circuit (ceiling)
Ceiling middle to load circuit (ceiling)	$R_{CM \rightarrow LC}$	T/E/time	Total thermal resistance between ceiling middle and load circuit (ceiling)
Outside to walls interface	$R_{OSA \rightarrow W}$	T/E/time	Total thermal resistance between outside air and walls
Outside to attic interface	$R_{OSA \rightarrow CA}$	T/E/time	Total thermal resistance between outside air and attic
Solar Gain Factor for Z1	$F_{SOL \rightarrow Z1}$	m^2	Solar Gain Factor
Solar Gain Factor for W	$F_{SOL \rightarrow W}$	m^2	Solar Gain Factor
Solar Gain Factor for Z2	$F_{SOL \rightarrow Z2}$	m^2	Solar Gain Factor

DYNAMIC SYSTEM EQUATIONS

Physical models utilized to develop dynamic equations include conservation of energy and simplified heat transfer between adjacent elements modeled as conduction.

$$\frac{d}{dt}(T_{LS}) = \frac{1}{R_{SB \rightarrow LS} C_{LS}} [T_{SB} - T_{LS}] - \frac{1}{C_{LS}} [Q_{LS}]$$

$$\frac{d}{dt}(T_E) = -\frac{1}{R_{E \rightarrow SB} C_E} [T_E - T_{SB}] - \frac{1}{R_{E \rightarrow FA} C_E} [T_E - T_{FA}] - \frac{1}{R_{E \rightarrow OSA} C_E} [T_E - T_{OSA}]$$

$$\frac{d}{dt}(T_{SB}) = \frac{1}{R_{SS \rightarrow SB} C_{SB}} [T_{SS} - T_{SB}] + \frac{1}{R_{E \rightarrow SB} C_{SB}} [T_E - T_{SB}] - \frac{1}{R_{SB \rightarrow LS} C_{SB}} [T_{SB} - T_{LS}]$$

$$\frac{d}{dt}(T_{SS}) = \frac{1}{R_{Z1 \rightarrow SS} C_{SS}} [T_{Z1} - T_{SS}] - \frac{1}{R_{SS \rightarrow SB} C_{SS}} [T_{SS} - T_{SB}]$$

$$\frac{d}{dt}(T_{Z1}) = \frac{1}{R_{W \rightarrow Z1} C_{Z1}} [T_W - T_{Z1}] - \frac{1}{R_{Z1 \rightarrow Z2} C_{Z1}} [T_{Z1} - T_{Z2}] - \frac{1}{R_{Z1 \rightarrow SS} C_{Z1}} [T_{Z1} - T_{SS}] + \frac{F_{sol \rightarrow Z1}}{C_{Z1}} [Sol_{GH}]$$

$$\frac{d}{dt}(T_W) = \frac{1}{R_{OSA \rightarrow W} C_W} [T_{OSA} - T_W] + \frac{1}{R_{W \rightarrow Z1} C_W} [T_W - T_{Z1}] - \frac{1}{R_{W \rightarrow Z2} C_W} [T_W - T_{Z2}] + \frac{F_{sol \rightarrow W}}{C_W} [Sol_{GH}]$$

$$\frac{d}{dt}(T_{Z2}) = \frac{1}{R_{W \rightarrow Z2} C_{Z2}} [T_W - T_{Z2}] + \frac{1}{R_{Z1 \rightarrow Z2} C_{Z2}} [T_{Z1} - T_{Z2}] - \frac{1}{R_{Z2 \rightarrow CS} C_{Z2}} [T_{Z2} - T_{CS}] + \frac{F_{sol \rightarrow Z2}}{C_{Z2}} [Sol_{GH}]$$

$$\frac{d}{dt}(T_{CS}) = \frac{1}{R_{Z2 \rightarrow CS} C_{CS}} [T_{Z2} - T_{CS}] - \frac{1}{R_{CS \rightarrow CM} C_{CS}} [T_{CS} - T_{CM}]$$

$$\frac{d}{dt}(T_{CM}) = \frac{1}{R_{CS \rightarrow CM} C_{CM}} [T_{CS} - T_{CM}] + \frac{1}{R_{CA \rightarrow CM} C_{CM}} [T_{CA} - T_{CM}] - \frac{1}{R_{CM \rightarrow LC} C_{CM}} [T_{CM} - T_{LC}]$$

$$\frac{d}{dt}(T_{CA}) = \frac{1}{R_{OSA \rightarrow CA} C_{CA}} [T_{OSA} - T_{CA}] - \frac{1}{R_{CA \rightarrow CM} C_{CA}} [T_{CA} - T_{CM}]$$

$$\frac{d}{dt}(T_{LC}) = \frac{1}{R_{CM \rightarrow CL} C_{LC}} [T_{CM} - T_{LC}] - \frac{1}{C_{LC}} [Q_{LC}]$$

$$B = \begin{bmatrix} 0 & 0 & -1/C_{LS} & 0 & 0 \\ 1/R_{E \rightarrow OSA} C_E & 1/R_{E \rightarrow OSA} C_E & 0 & 0 & 0 \\ 0 & 0 & 0 & 0 & 0 \\ 0 & 0 & 0 & 0 & 0 \\ 0 & 0 & 0 & 0 & 0 \\ 1/R_{OSA \rightarrow W} C_W & 0 & 0 & 0 & 0 \\ 0 & 0 & 0 & 0 & 0 \\ 0 & 0 & 0 & 0 & 0 \\ 0 & 0 & 0 & 0 & 0 \\ 1/R_{OSA \rightarrow CA} C_{CA} & 0 & 0 & 0 & 0 \\ 0 & 0 & 0 & -1/C_{LC} & 0 \end{bmatrix} \begin{matrix} \\ \\ \\ F_{sol \rightarrow Z1}/C_{Z1} \\ F_{sol \rightarrow W}/C_W \\ F_{sol \rightarrow Z2}/C_{Z2} \\ \\ \\ \\ \\ \end{matrix}$$

$$\begin{bmatrix} X_1 \\ X_2 \\ X_3 \\ X_4 \\ X_5 \\ X_6 \\ X_7 \\ X_8 \\ X_9 \\ X_{10} \\ X_{11} \end{bmatrix} = \begin{bmatrix} T_{LS}(t) \\ T_E(t) \\ T_{SB}(t) \\ T_{SS}(t) \\ T_{Z1}(t) \\ T_W(t) \\ T_{Z2}(t) \\ T_{CS}(t) \\ T_{CM}(t) \\ T_{CA}(t) \\ T_{LC}(t) \end{bmatrix}$$

$$\begin{bmatrix} U_1 \\ U_2 \\ U_3 \\ U_4 \\ U_5 \end{bmatrix} = \begin{bmatrix} T_{OSA}(t) \\ T_{FA}(t) \\ Q_{LS}(t) \\ Q_{LC}(t) \\ Sol_{GH}(t) \end{bmatrix}$$

LINEAR IN THE PARAMETERS REPRESENTATION

The dynamic equations for each node in linear in the parameters form, $z(t) = \theta * \varphi(t)$.

$$\theta_{T_{LS}} = \left[\left(\frac{1}{R_{SB \rightarrow LS} C_{LS}} \right) \left(-\frac{1}{C_{LS}} \right) \right]$$

$$\varphi_{T_{LS}} = \begin{bmatrix} T_{SB} - T_{LS} \\ Q_{LS} \end{bmatrix}$$

$$\theta_{T_E} = \left[\left(-\frac{1}{R_{E \rightarrow SB} C_E} \right) \left(-\frac{1}{R_{E \rightarrow FA} C_E} \right) \left(-\frac{1}{R_{E \rightarrow OSA} C_E} \right) \right]$$

$$\varphi_{T_E} = \begin{bmatrix} T_E - T_{SB} \\ T_E - T_{FA} \\ T_E - T_{OSA} \end{bmatrix}$$

$$\theta_{T_{SB}} = \left[\left(\frac{1}{R_{SS \rightarrow SB} C_{SB}} \right) \left(\frac{1}{R_{E \rightarrow SB} C_{SB}} \right) \left(-\frac{1}{R_{SB \rightarrow LS} C_{SB}} \right) \right]$$

$$\varphi_{T_{SB}} = \begin{bmatrix} T_{SS} - T_{SB} \\ T_E - T_{SB} \\ T_{SB} - T_{LS} \end{bmatrix}$$

$$\theta_{T_{SS}} = \left[\left(\frac{1}{R_{Z1 \rightarrow SS} C_{SS}} \right) \left(-\frac{1}{R_{SS \rightarrow SB} C_{SS}} \right) \right] \quad \varphi_{T_{SS}} = \begin{bmatrix} T_{Z1} - T_{SS} \\ T_{SS} - T_{SB} \end{bmatrix}$$

$$\theta_{T_{Z1}} = \left[\left(\frac{1}{R_{W \rightarrow Z1} C_{Z1}} \right) \left(-\frac{1}{R_{Z1 \rightarrow Z2} C_{Z1}} \right) \left(-\frac{1}{R_{Z1 \rightarrow SS} C_{Z1}} \right) \left(\frac{F_{sol \rightarrow Z1}}{C_{Z1}} \right) \right] \quad \varphi_{T_{Z1}} = \begin{bmatrix} T_W - T_{Z1} \\ T_{Z1} - T_{Z2} \\ T_{Z1} - T_{SS} \\ Sol_{GH} \end{bmatrix}$$

$$\theta_{T_W} = \left[\left(\frac{1}{R_{OSA \rightarrow W} C_W} \right) \left(\frac{1}{R_{W \rightarrow Z1} C_W} \right) \left(-\frac{1}{R_{W \rightarrow Z2} C_W} \right) \left(\frac{F_{sol \rightarrow W}}{C_W} \right) \right] \quad \varphi_{T_W} = \begin{bmatrix} T_{OSA} - T_W \\ T_W - T_{Z1} \\ T_W - T_{Z2} \\ Sol_{GH} \end{bmatrix}$$

$$\theta_{T_{Z2}} = \left[\left(\frac{1}{R_{W \rightarrow Z2} C_{Z2}} \right) \left(\frac{1}{R_{Z1 \rightarrow Z2} C_{Z2}} \right) \left(-\frac{1}{R_{Z2 \rightarrow CS} C_{Z2}} \right) \left(\frac{F_{sol \rightarrow Z2}}{C_{Z2}} \right) \right] \quad \varphi_{T_{Z2}} = \begin{bmatrix} T_W - T_{Z2} \\ T_{Z2} - T_{CS} \\ T_{Z1} - T_{Z2} \\ Sol_{GH} \end{bmatrix}$$

$$\theta_{T_{CS}} = \left[\left(\frac{1}{R_{Z2 \rightarrow CS} C_{CS}} \right) \left(-\frac{1}{R_{CS \rightarrow CM} C_{CS}} \right) \right] \quad \varphi_{T_{CS}} = \begin{bmatrix} T_{Z2} - T_{CS} \\ T_{CS} - T_{CM} \end{bmatrix}$$

$$\theta_{T_{CM}} = \left[\left(\frac{1}{R_{CS \rightarrow CM} C_{CM}} \right) \left(\frac{1}{R_{CA \rightarrow CM} C_{CM}} \right) \left(-\frac{1}{R_{CM \rightarrow LC} C_{CM}} \right) \right] \quad \varphi_{T_{CM}} = \begin{bmatrix} T_{CS} - T_{CM} \\ T_{CA} - T_{CM} \\ T_{CM} - T_{CM} \end{bmatrix}$$

$$\theta_{T_{CA}} = \left[\left(\frac{1}{R_{OSA \rightarrow CA} C_{CA}} \right) \left(-\frac{1}{R_{CA \rightarrow CM} C_{CA}} \right) \right] \quad \varphi_{T_{CA}} = \begin{bmatrix} T_{OSA} - T_{CA} \\ T_{CA} - T_{CM} \end{bmatrix}$$

$$\theta_{T_{LC}} = \left[\left(\frac{1}{R_{CM \rightarrow CL} C_{LC}} \right) \left(-\frac{1}{C_{LC}} \right) \right] \quad \varphi_{T_{LC}} = \begin{bmatrix} T_{CM} - T_{LC} \\ Q_{LC} \end{bmatrix}$$

Table 3: Parameter Identification Results

Phi $\Phi(t)$	Parameter Estimates θ	Initial Guess θ_0	Initial θ estimate	Final θ
$\varphi_{T_{LS}}$	$\hat{\theta}_{T_{LS}}(1)$	0.1	0.1052	0.2052
	$\hat{\theta}_{T_{LS}}(2)$	-0.1	-0.0037	-0.005
	$\hat{\theta}_{T_E}(1)$	-0.1	-2.53E-05	-2.53E-05
$\varphi_{T_{LS}}$	$\hat{\theta}_{T_E}(2)$	-0.1	-0.0050	-0.005
	$\hat{\theta}_{T_E}(3)$	-0.1	-3.84E-04	-3.84E-04

$\varphi_{T_{LS}}$	$\hat{\theta}_{T_{SB}}(1)$	0.1	0.0299	0.0299
	$\hat{\theta}_{T_{SB}}(2)$	0.1	-3.37E-04	1.00E-04
	$\hat{\theta}_{T_{SB}}(3)$	-0.1	-0.0078	-0.01
$\varphi_{T_{LS}}$	$\hat{\theta}_{T_{SS}}(1)$	0.1	0.0043	0.0043
	$\hat{\theta}_{T_{SS}}(2)$	-0.1	-0.0368	-0.0368
$\varphi_{T_{LS}}$	$\hat{\theta}_{T_{Z1}}(1)$	0.1	0.0087	0.007
	$\hat{\theta}_{T_{Z1}}(2)$	-0.1	-0.0321	-0.0321
	$\hat{\theta}_{T_{Z1}}(3)$	-0.1	-0.0120	-0.0120
	$\hat{\theta}_{T_{Z1}}(4)$	0.1	3.72E-05	3.72E-05
$\varphi_{T_{LS}}$	$\hat{\theta}_{T_W}(1)$	0.1	0.0012	0.0012
	$\hat{\theta}_{T_W}(2)$	-0.1	0.0013	-8.00E-05
	$\hat{\theta}_{T_W}(3)$	-0.1	0.0028	-0.001
	$\hat{\theta}_{T_W}(4)$	0.1	3.07E-05	3.07E-05
$\varphi_{T_{LS}}$	$\hat{\theta}_{T_{Z2}}(1)$	0.1	0.0051	0.0045
	$\hat{\theta}_{T_{Z2}}(2)$	-0.1	-0.0071	-0.03
	$\hat{\theta}_{T_{Z2}}(3)$	0.1	0.0155	0.0155
	$\hat{\theta}_{T_{Z2}}(4)$	0.1	4.79E-04	4.79E-05
$\varphi_{T_{LS}}$	$\hat{\theta}_{T_{CS}}(1)$	0.1	-0.0016	1.00E-02
	$\hat{\theta}_{T_{CS}}(2)$	-0.1	9.47E-04	-0.005
$\varphi_{T_{LS}}$	$\hat{\theta}_{T_{CM}}(1)$	0.1	0.0369	0.019
	$\hat{\theta}_{T_{CM}}(2)$	0.1	6.10E-04	6.10E-05
	$\hat{\theta}_{T_{CM}}(3)$	-0.1	-0.0150	-0.015
$\varphi_{T_{LS}}$	$\hat{\theta}_{T_{CA}}(1)$	0.001	0.0044	0.0044
	$\hat{\theta}_{T_{CA}}(2)$	-0.001	9.00E-04	-1.00E-05
$\varphi_{T_{LS}}$	$\hat{\theta}_{T_{LC}}(1)$	0.1	0.0985	0.08
	$\hat{\theta}_{T_{LC}}(2)$	-0.1	-0.0099	-0.006

BASELINE CONDITIONS:

We have collected minute increment measurements for over 150 points of information from the Honda Smart Home since June 2014. Our project reported here will use data from 2015, a period of time for which data has been vetted and observed and when the home was operating regularly with occupants. Most importantly, each of the state variables in our draft model, and most of the input variables, are available in the dataset. The deep earth temperature is not measured, per se, so our modeling will assume a constant 65°F. We calculated the data for sensible cooling delivered by fluid in the slab and ceiling load circuit, Q_{LS} and Q_{LC} , as the difference in temperature supplied and temperature returned times the mass flow rate and specific heat capacity of the water. We chose August as a one-month set for the training data, used for parameter identification, and September as validation data, used to compare the system model to actual state measurements.

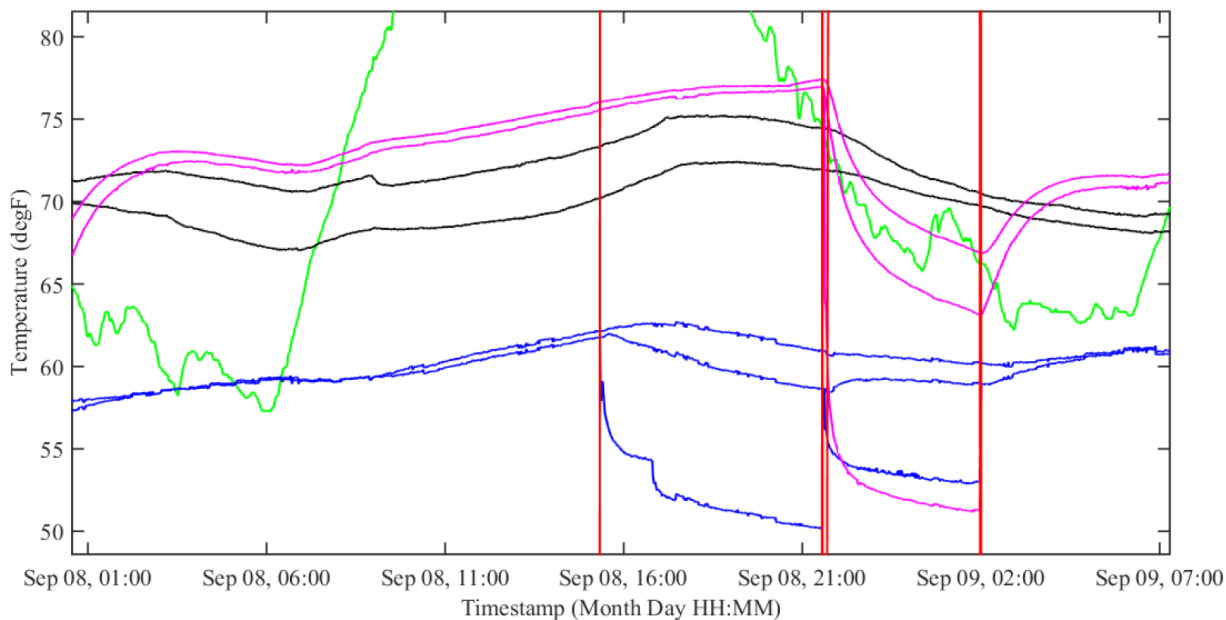


Figure: Time series plot of zone temperatures (black), ceiling temperatures (magenta), and slab temperatures for one day of normal operation. Cooling mode is bounded by the red vertical lines. Cooling was activated at about 3:00 pm on Sep 08, after the zone temperature rose above the comfort setpoint. Cooling operated continuously for 11 hours before the setpoint was satisfied.

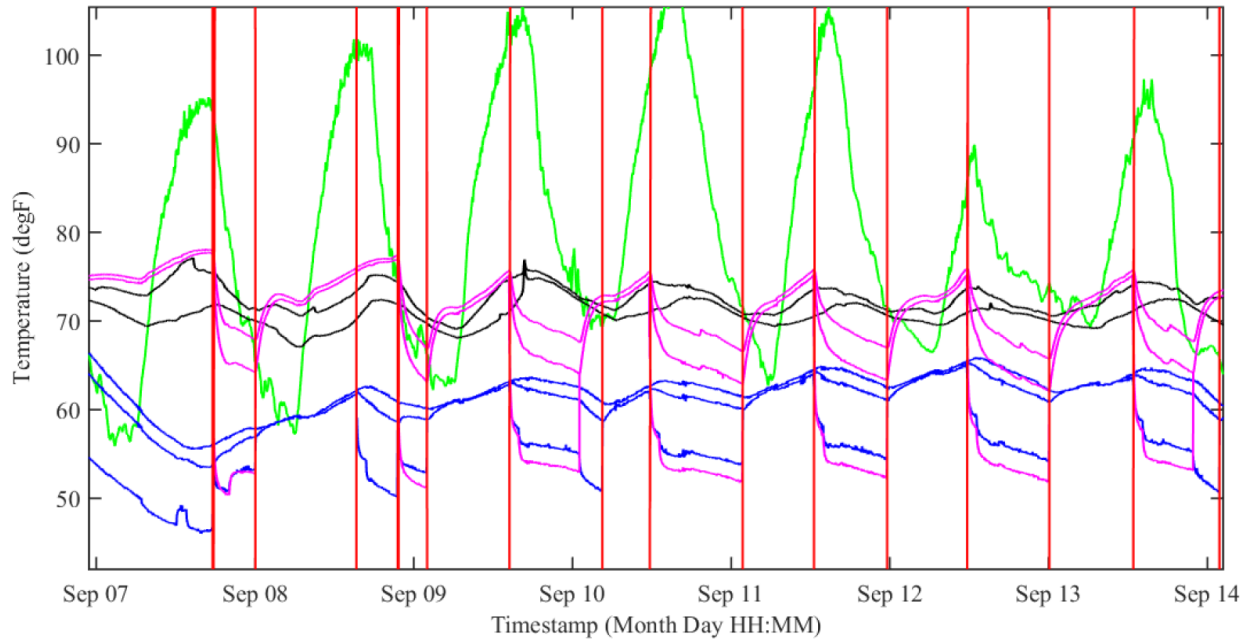


Figure: Time series plot of zone temperatures (black), ceiling temperatures (magenta), and slab temperatures for one day of normal operation. Cooling mode is bounded by the red vertical lines. Cooling operates for several hours at a time. By the time that the zone temperature is satisfied the slab has been over cooled. Release of the stored cooling energy over the next several hours continues to cool the zone overnight, when nighttime ventilation cooling could be used instead.

RESULTS

PARAMETER IDENTIFICATION

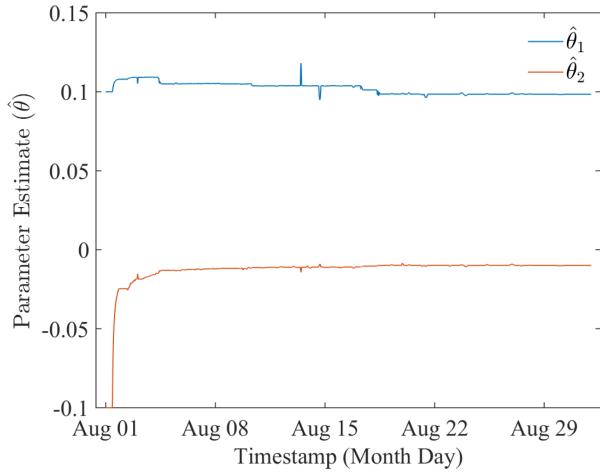


Figure: Parameter estimates for $d/dt T_{LS}$

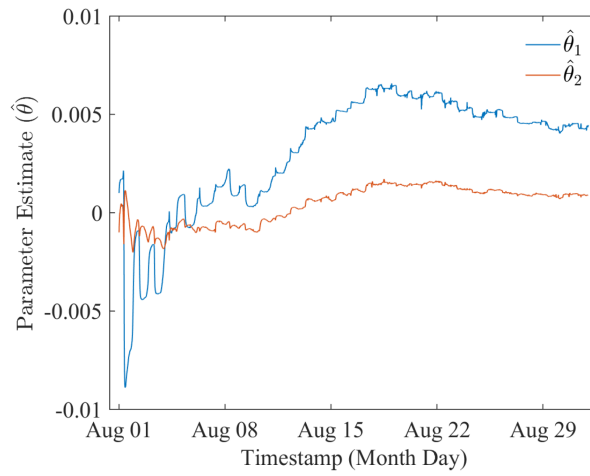


Figure: Parameter estimates for $d/dt T_{CA}$

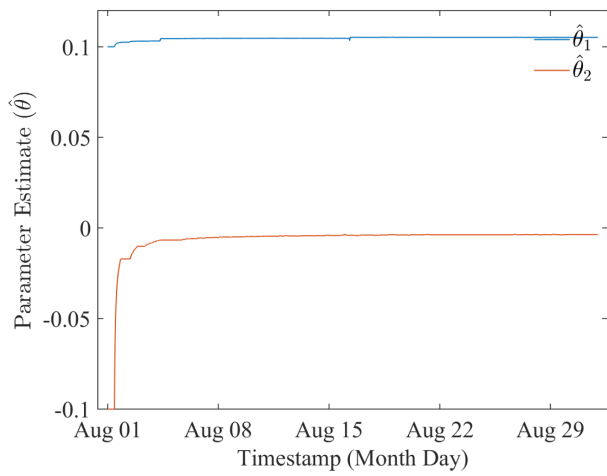


Figure: Parameter estimates for $d/dt T_{LC}$

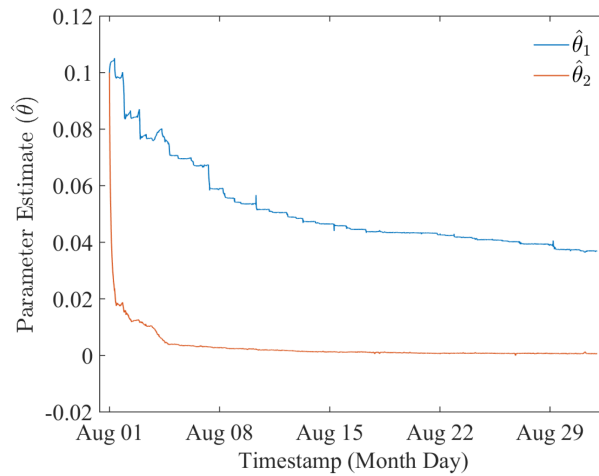
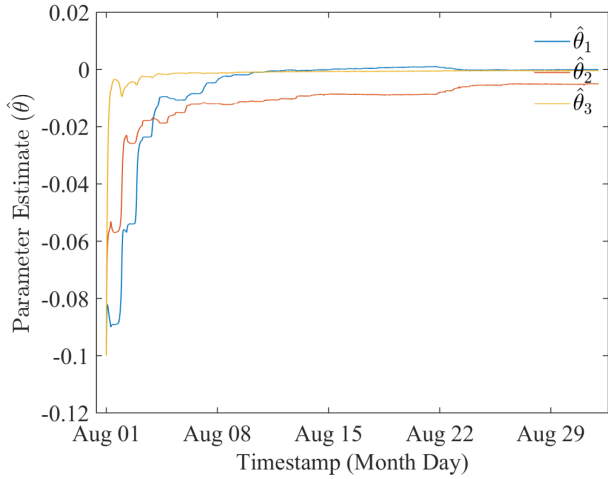


Figure: Parameter estimates for $d/dt T_{CM}$



Parameter estimates for: $d/dt T_E$

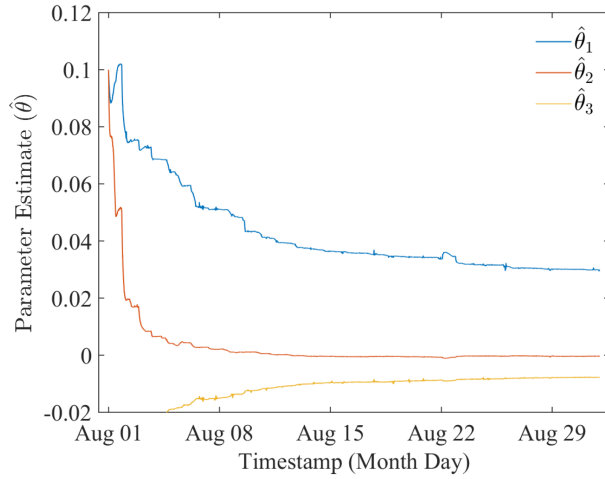


Figure: Parameter estimates for: $d/dt T_{SB}$

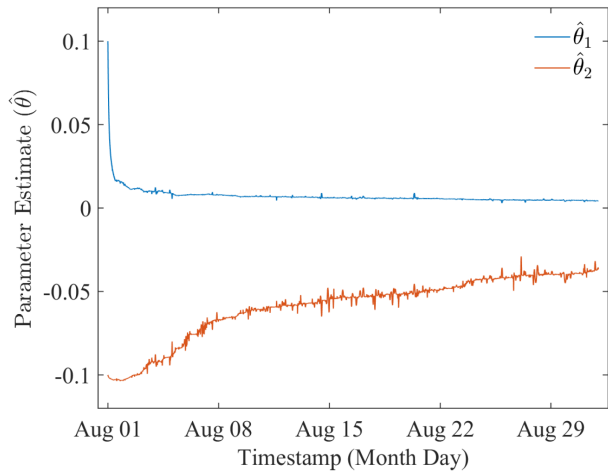


Figure: parameter estimates for: $d/dt T_{SS}$

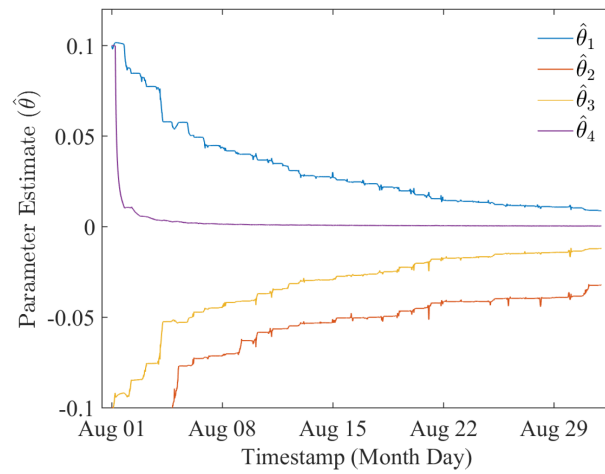


Figure: Parameter estimates for $d/dt T_{Z1}$

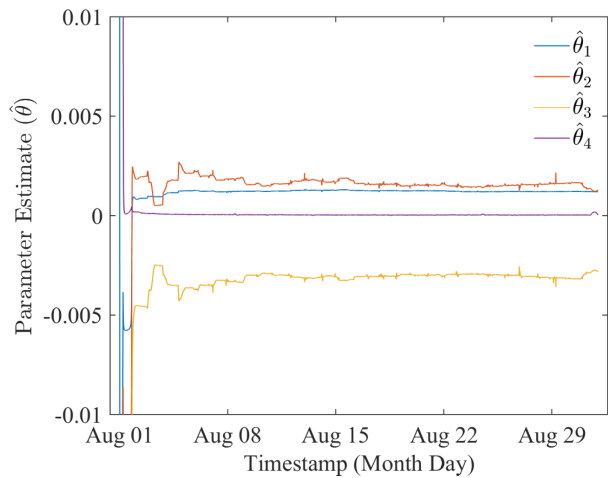


Figure: Parameter estimates for: $d/dt T_W$

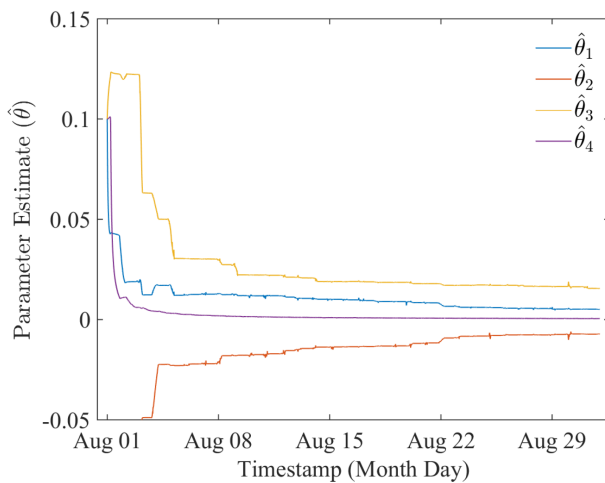


Figure: Parameter estimates for: $d/dt T_{Z2}$

VALIDATION OF DYNAMIC SIMULATION WITH OUT-OF-SAMPLE SET

Time series comparisons of particular states. Separate plots for room, slab, ceiling temperatures, etc.

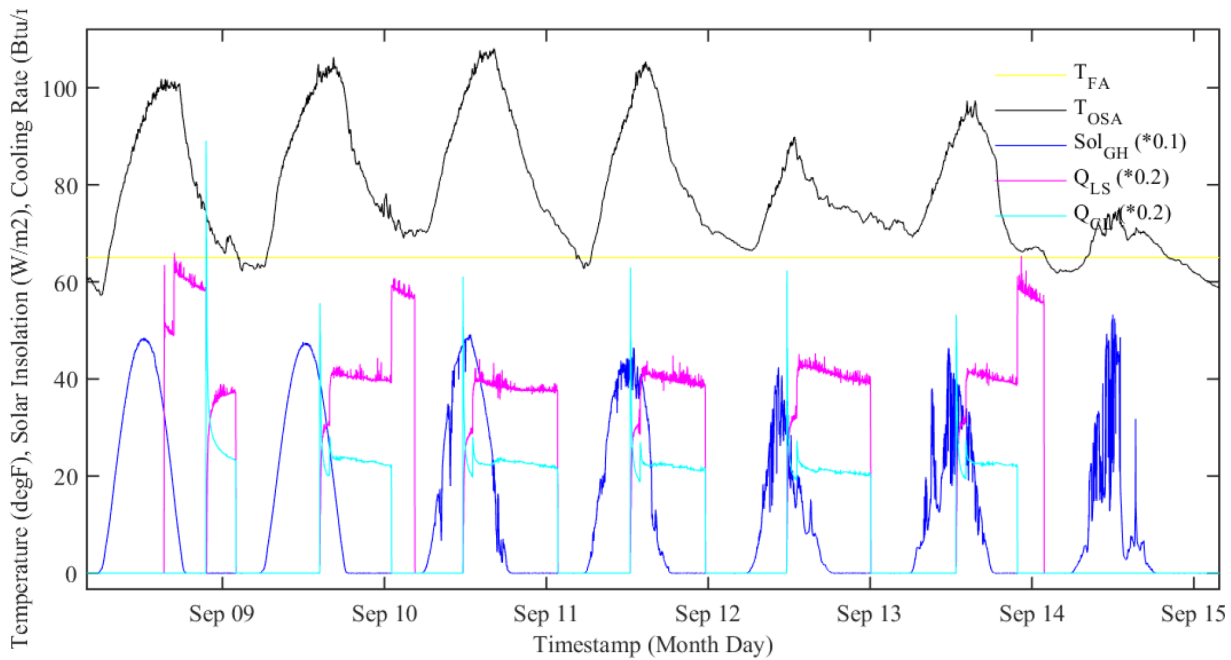


Figure: One week of uncontrolled input data from an out-of-sample validation data set. Outside air temperature (black), far earth temperature (yellow), slab cooling rate (magenta), ceiling cooling rate (cyan), and solar insolation (blue) were measured on site. For simulation of alternate control strategies, the slab cooling rate and ceiling cooling rate would be treated as controlled input variables.

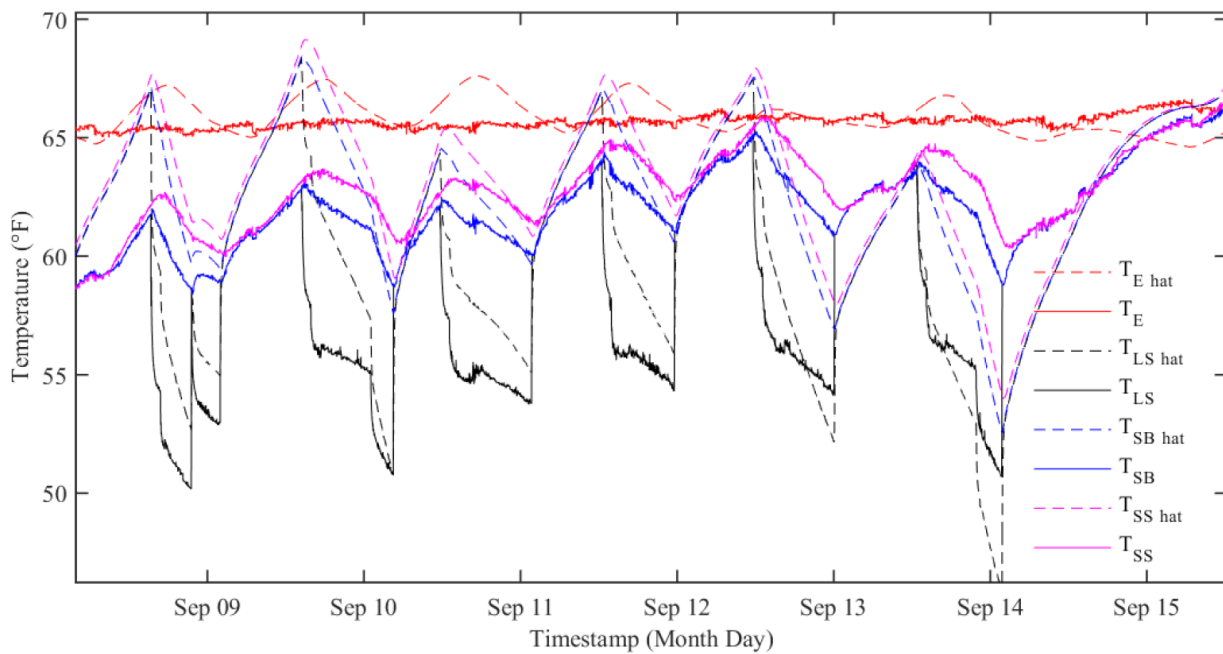


Figure: Comparison of slab temperature predictions (dashed lines) to measured states (solid lines) for one week in an out of sample data period. The predictions for earth temperature immediately below the slab (red), the average slab chilled water temperature (black), slab bottom temperature (blue), and slab surface temperature (magenta), are normally within $\pm 5^\circ\text{F}$ during cooling operation.

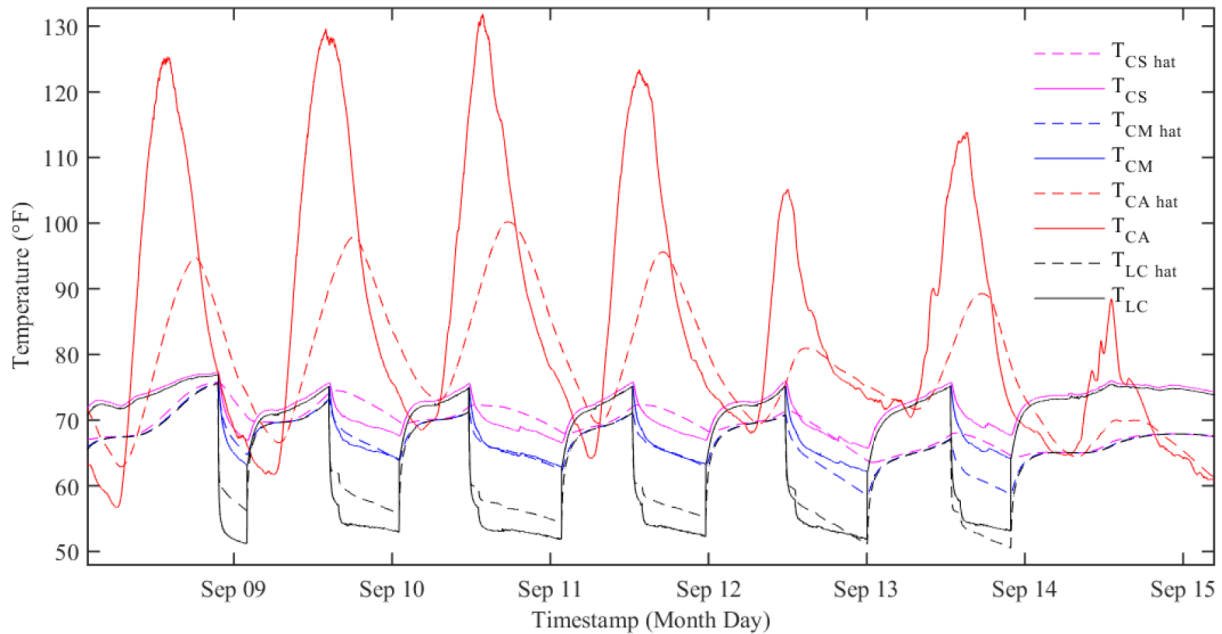


Figure: Comparison of ceiling temperature predictions (dashed lines) to measured states (solid lines) for one week in an out of sample data period. The predictions for average ceiling chilled water temperature (black), ceiling middle temperature (blue), and ceiling surface temperature (magenta) are always within $\pm 5^\circ\text{F}$.

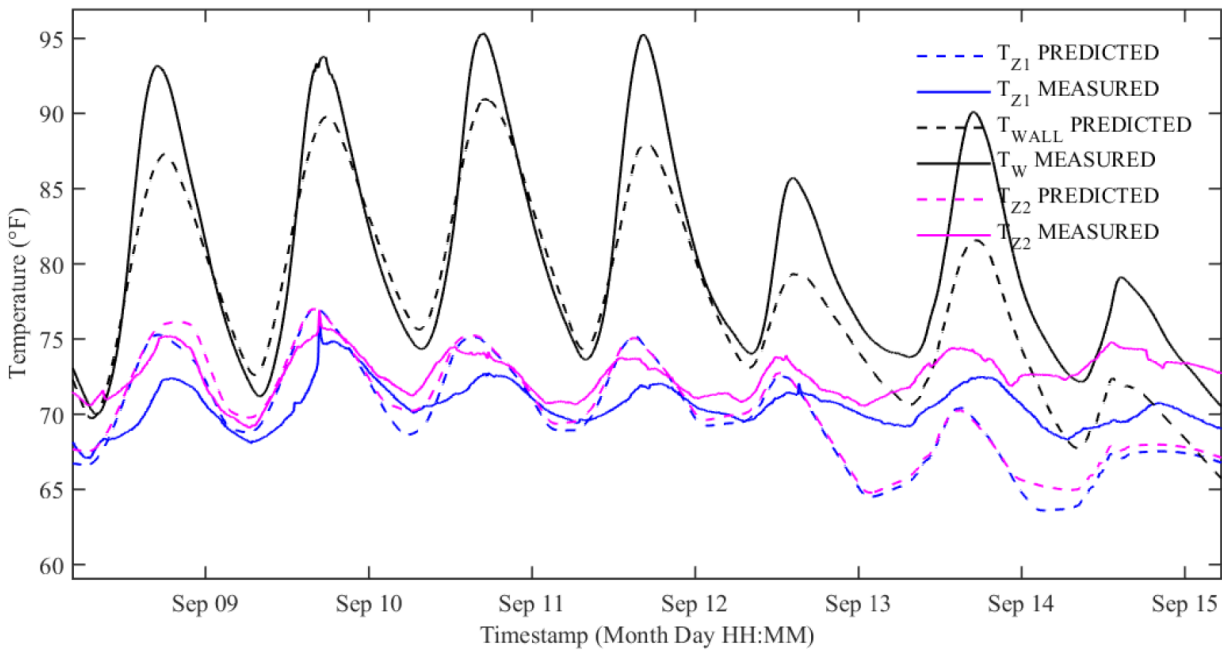


Figure: Comparison of zone temperature predictions (dashed lines) to measured states (solid lines) for one week in an out of sample data period. The predictions for first floor zone temperature (blue) and second floor zone temperature (magenta) are always within $\pm 5^\circ\text{F}$ of measured temperatures. The prediction for wall temperature varies from measurements by a larger margin.

CONCLUSIONS

From this project, we learned both about the thermal dynamic model of radiant cooling in the Honda Smart Home and about the method for adopting it. We also identified future directions for further parameter identification work and possible avenues for optimization.

Our simulation results that compare estimated state temperature to measured state temperature vary within a $\pm 5^\circ\text{F}$ margin for the two zones, slab, and ceiling surfaces. The accuracy of the attic and wall temperature vary more widely up to $\pm 10^\circ\text{F}$. With the intention that future work could improve upon results, we analyze the modeling and parametric identification methods:

- *Modeling:* Certain heat transfer mechanisms that are not accounted for in our model could be affecting the state temperature predictions. For example, the attic temperature was not linked to solar radiation. It is possible if that link was tied into the energy balance equation for the attic, its temperature would be more accurately predicted. Additionally, it is also possible that the model considered too many factors and by doing so, introduced relationships that do not fully describe the interactions for all states. However, we also used this data to estimate parameters for a much simpler dynamic model, with 3 states and 2 inputs, which was prone to the same errors. The choice of which states and inputs were used in the simpler model could also be reevaluated/ further explored. Much care is required in careful selection of the nodes and links considered in such a model.
- *Parametric Identification:* Our predictions can be improved through further iterations of the parameters and the use of more data. By initializing the least square algorithm with parameter estimates, the simulations appear to be more accurate and would benefit from more iterations. To what sensitivity the nodes are linked, to what degree the parameters influence the heat exchange, is the crucial search in this modeling process. In our model, for instance, we are less interested in attic temperature as we are zone temperature, but the coupling of the attic temperature to the ceiling middle to the ceiling surface and so on is impacted. We saw improvements in our simulation upon refining our parameters, but more could be done to lessen the $\pm 5^\circ\text{F}$ margin. Furthermore, parameter estimation can result in values that cause instability in the dynamic simulations. Parameter estimates that violate physical principles indicate that the structure our dynamic model may not take into account all relevant factors.

REFERENCES

- Afram, Abdul, and Farrokh Janabi-Sharifi. 2014. "Theory and Applications of HVAC Control Systems – A Review of Model Predictive Control (MPC)." *Building and Environment* 72 (February): 343–55. doi:10.1016/j.buildenv.2013.11.016.
- ASHRAE Handbook. HVAC Systems and Equipment 2012. Chapter 13. Hydronic Heating and Cooling.
- ASHRAE Handbook. HVAC Systems and Equipment 2008. Chapter 12. Hydronic Heating and Cooling System Design.
- Ferkl, Lukáš, and Jan Široký. 2010. "Ceiling Radiant Cooling: Comparison of ARMAX and Subspace Identification Modelling Methods." *Building and Environment* 45 (1): 205–12.
- Prívvara, Samuel, Jan Široký, Lukáš Ferkl, and Jiří Cigler. 2011. "Model Predictive Control of a Building Heating System: The First Experience." *Energy and Buildings* 43 (2-3): 564–72.
- Stetiu, Corina. 1999. "Energy and Peak Power Savings Potential of Radiant Cooling Systems in US Commercial Buildings." *Energy and Buildings* 30 (2): 127–38.
- U.S. Department of Energy, Energy Efficiency and Renewable Energy. "2011 Buildings Energy Data Book." D&R International, Ltd., March 2012. <http://buildingsdatabook.eren.doe.gov/>.